ISTITUTO NAZIONALE DI FISICA NUCLEARE

Sezione di Torino

INFN/BE-70/8
16 Ottobre 1970

G. C. Bonazzola, T. Bressani, E. Chiavassa, L. Pasqualini, C. Rubbia and G. Venturello: PROPOSAL OF AN EXPERIMENTAL SET-UP FOR THE STUDY OF HYPERNUCLEI IN FLIGHT. -

133

Reparto Tipografico
dei Laboratori Nazionali di Frascati

Istituto Nazionale di Fisica Nucleare
Sezione di Torino

INFN/BE-70/8
16 Ottobre 1970

G.C. Bonazzola, T. Bressani, E. Chiavassa, L. Pasqualini, C. Rubbia(x) and G. Venturello: PROPOSAL OF AN EXPERIMENTAL SET-UP FOR THE STUDY OF HYPERNUCLEI IN FLIGHT. -

1. - INTRODUCTION. -

In this report we give more details about the experiment[1,2] planned to study hypernuclear states with the reaction

$$K^- + (\text{nucleus}) \rightarrow (\text{hypernucleus}) + \pi^- \qquad (1)$$

with K^- in flight and π^- detected at forward angles.

We emphasize that the main advantage of using K^- in flight instead of at rest is that the Λ produced in the free reaction

$$K^- + n \rightarrow \Lambda + \pi^- \qquad (2)$$

has a smaller momentum for π^- detected at forward angles ($\sim$50 MeV/c). Feshbach and Kerman[3] and Dalitz[4] have pointed out that the reaction (1) is a powerful tool to investigate the symmetry of the nuclear wave functions, and we refer to these works for details.

(x) - CERN, Geneva, Switzerland - Present address: Department of Physics, Harvard University, Cambridge, Mass. 02138 (USA).

2. - EXPERIMENTAL SET-UP. -

2.1. - Beam. -

We plan to use the actual k_{12} beam of the CERN PS in the short version[5] and we have designed our set-up for its features.

The maximum K^- momentum of this beam is 550 MeV/c. From the kinematics[2] we see that the π^- arising from reaction (1) have $\sim$ 550 MeV/c as well[x]. It is obviously unacceptable that they should have the same momentum as the π^- contamination of the K^- beam, and it is imperative to choose an incident K^- momentum for which the π^- from reaction (1) has a different momentum from the incident momentum. We propose to work with K^- of 400 MeV/c, for which the π^- from reaction (1) has a momentum of 430 MeV/c.

2.2- Magnet. -

The actual experimental area allocated to the k_{12} beam is very small. Therefore we made an effort to find an experimental set-up that was as compact as possible. The first idea was to use two bending magnets, each 1 m long, the first one to analyse the incoming K^- momentum and the second the outgoing π^-. The same result can be achieved by using a single magnet with a gap length of 2 m and the target in the middle. A suitable magnet, already in existence at CERN, is the modified 2 m magnet; it has a pole spacing of 30 cm and coils which allow a maximum field of $\sim$12 kG. Because the cross-section of the incoming K^- beam is much smaller than 30 cm, we reduce the gap in the first part of the magnet to $\sim$ 15 cm in order to obtain, with the maximum allowed current of 880 A, a field of $\sim$ 18.0 kG. For the outgoing π^- the actual gap of 30 cm is maintained in order to ensure a greater solid angle. Figure 1 gives the shape and the size of the shims in the first part of the magnet. Owing to the greater bending power of the first part of the magnet, the target will be placed in an eccentric position. In Fig. 1 we have drawn some limiting trajectories for the particles in the magnet.

The actual experimental area will be large enough for our purposes. However, if for some particular reason the allocated space has to be reduced, this can be achieved by erecting the magnet in a vertical position.

2.3. - Multiwire proportional counters (MPWC). -

We will localize the K^- and the π^- in front of, inside, and at the back of the magnet with a set of eight pairs of MPWC. The use of MPWC

(x) - We note that the momenta of the π^- emitted in reaction (1) have values close to the values of the free reaction (2), apart from the differences between the binding energy of the neutron in the nucleus and the Λ in the hypernucleus.

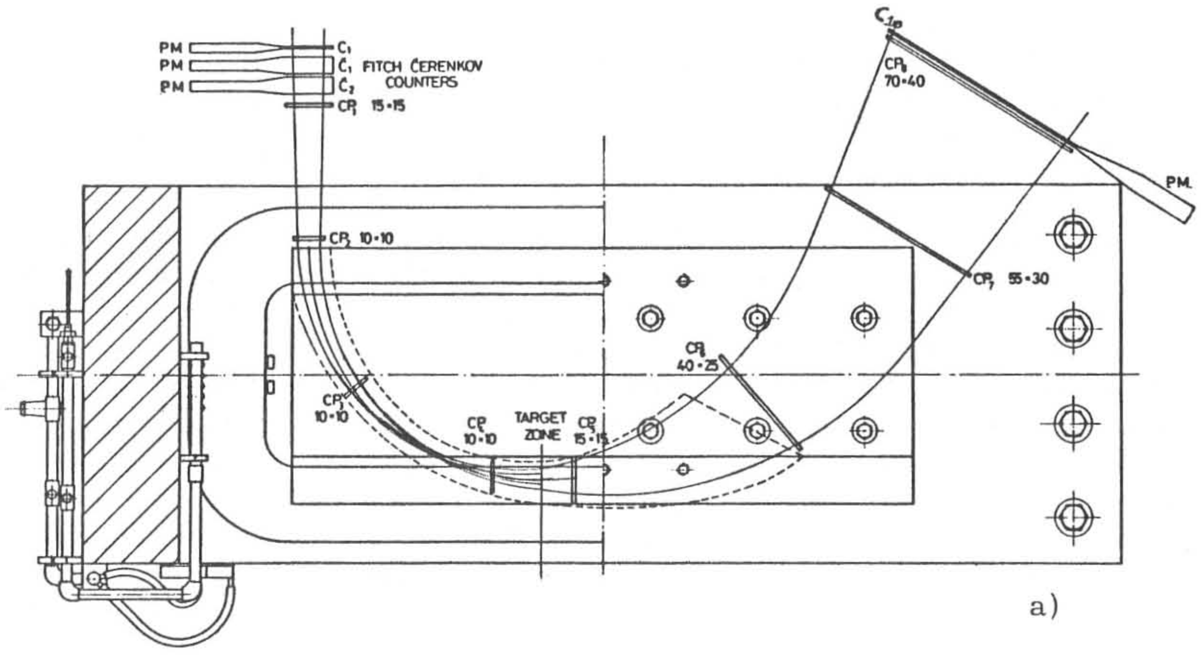

a)

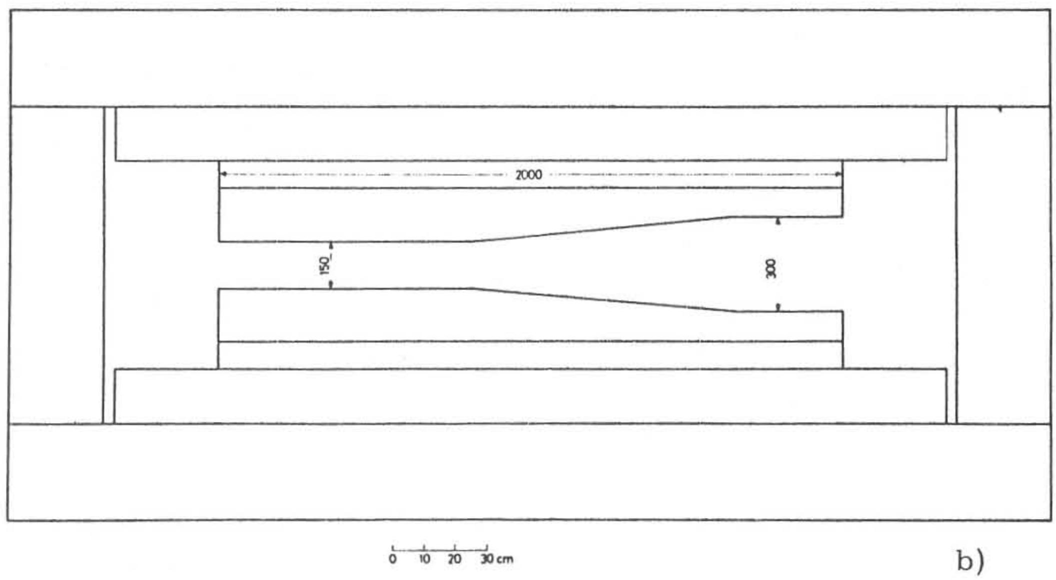

b)

FIG. 1 - a) Plant view of the magnet: some limiting trajectories of the particles are indicated, together with the positions and the dimensions of the MPWC; the dotted line represents the shims of the magnetic poles; the target zone is detailed in Fig. 4.
b) Section of the magnet.

is dictated by the intense beam and by the fact that they must be used inside the magnet. Taking into account the limiting trajectories sketched in Fig. 1, we obtained the dimensions of the chambers; these are given in the same figure. We see that $\sim$1750 activated wires will be required for a wire spacing of 2 mm. Hence an effort is being made to find a system that is capable of reducing the number of amplifiers[6].

Because we will record only one event for each chamber at a time, we found that it is possible to identify each of the N wires of a chamber as an element of a square matrix of dimension $\sqrt{N}$. There is an electronic channel corresponding to each row and column of the matrix, and every wire of the chamber is connected to the inputs of the corresponding row and column amplifiers. In this way, only $2\sqrt{N}$ channels are needed for identifying each wire[x]. In the case where two or more wires are fired, ambiguities are encountered. In some of the cases they can be removed by looking at several chambers. This method was proposed by Pizer[7] for wire spark chambers, and applied to proportional wire chambers by Charpak et al.[8] using pulse transformers for mixing the signals. The same idea may be implemented as follows.

In Fig. 2 let us suppose that the wires of a row are connected through the resistors R to the input of a mixing amplifier. The input impedance r must be much smaller than R. Each wire is also connected through an identical resistor R to the column amplifier.

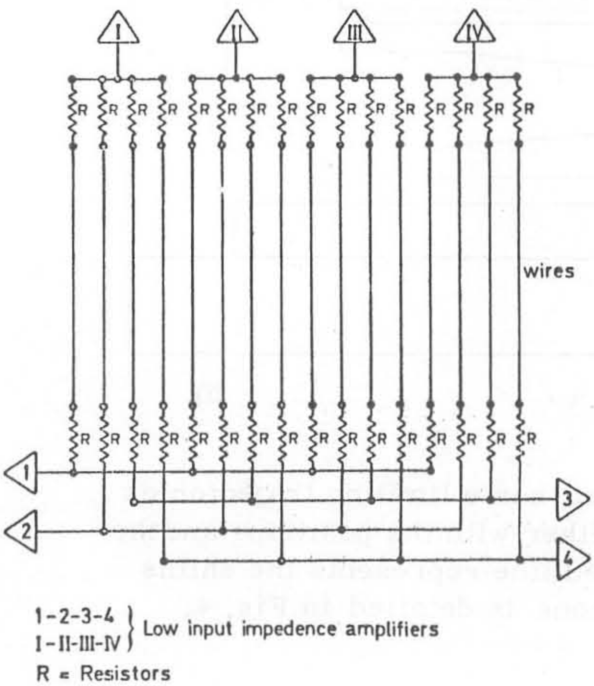

FIG. 2 - An example of the proposed coding system for a counter with N = 16 wires. The amplifiers labelled, I, II, III, IV give the column number a; those labelled as 1, 2, 3, 4 the row number b.

(x) - The usual order number of the wires is obviously given by $\left[(a-1)\sqrt{N}+b\right]$.

Calling i the current flowing in a counting wire, we can immediately calculate that the two amplifiers connected to the wire will collect a current $i(2R+r)/2(2R+\sqrt{N}r)$. All remaining amplifiers will receive, at the same time, a feedthrough current $ir/2(2R+\sqrt{N}r)$. By choosing optimal values for the resistors R, the input impedance r, and the threshold of the logic, it is possible to get signals only from the correct channels.

Tests of the proposed system were performed using a multiwire proportional counter with sixteen wires, connected into subgroups of four. The mixing amplifier was a BSX 29 transistor connected in common base configuration; the input impedance is $20\,\Omega$. The resistors R have values of $1.2\ k\Omega$, and the current flowing in the wires was of the order of $5\,\mu A$. The eight outputs were sent to eight channels consisting of a linear amplifier, a threshold detector, and a logic output system[9].

We tested the operation of this arrangement by irradiating one wire with a collimated β-source of ^{144}Ce, and putting a needle scintillator, placed under the irradiated wire in coincidence with the output of the doubles coincidences between the various combinations of row and column amplifiers.

Histograms (a) and (b) in Fig. 3 show the respective counting rates measured on the different wires when wires 11 and 8 are irradiated. As one can see in the figure, there is an appreciable counting rate also in adjacent wires. This counting rate could be due to physical effects, e.g. electron backscattering, or to incorrect operation of our system. To test this, we used the same geometry but connected one wire at a time to the row and column amplifiers. The results of this measurement are shown by a dotted line in Fig. 3b.

Since the two measurements on wire 8 almost coincide, we conclude that no feedthrough is present in our system.

A disadvantage of the proposed method with respect to the use of an amplifier for each wire, is that the probability of losing an event during the recovery time of the electronics is increased by a factor $\sqrt{N}$ where a uniform flux irradiates the counter. Hence this method can be very useful for large-area counters, where the flux of the impinging particles is not very high, and where the reduction of the number of amplifiers is very attractive. In some particular cases, such as when the flux of particles impinging on the counter is very intense only in a limited zone, the difficulty mentioned can be overcome by grouping the wires in a different way, i.e. one wire of the zone where the flux is very intense with ($\sqrt{N}$-1) wires that are not adjacent. Alternatively, in the zone of intense flux one can use separate amplifiers on each wire.

With this method, and taking into account the dimensions of the chambers of Fig. 1, the number of amplifiers will be reduced from 1750 to 338.

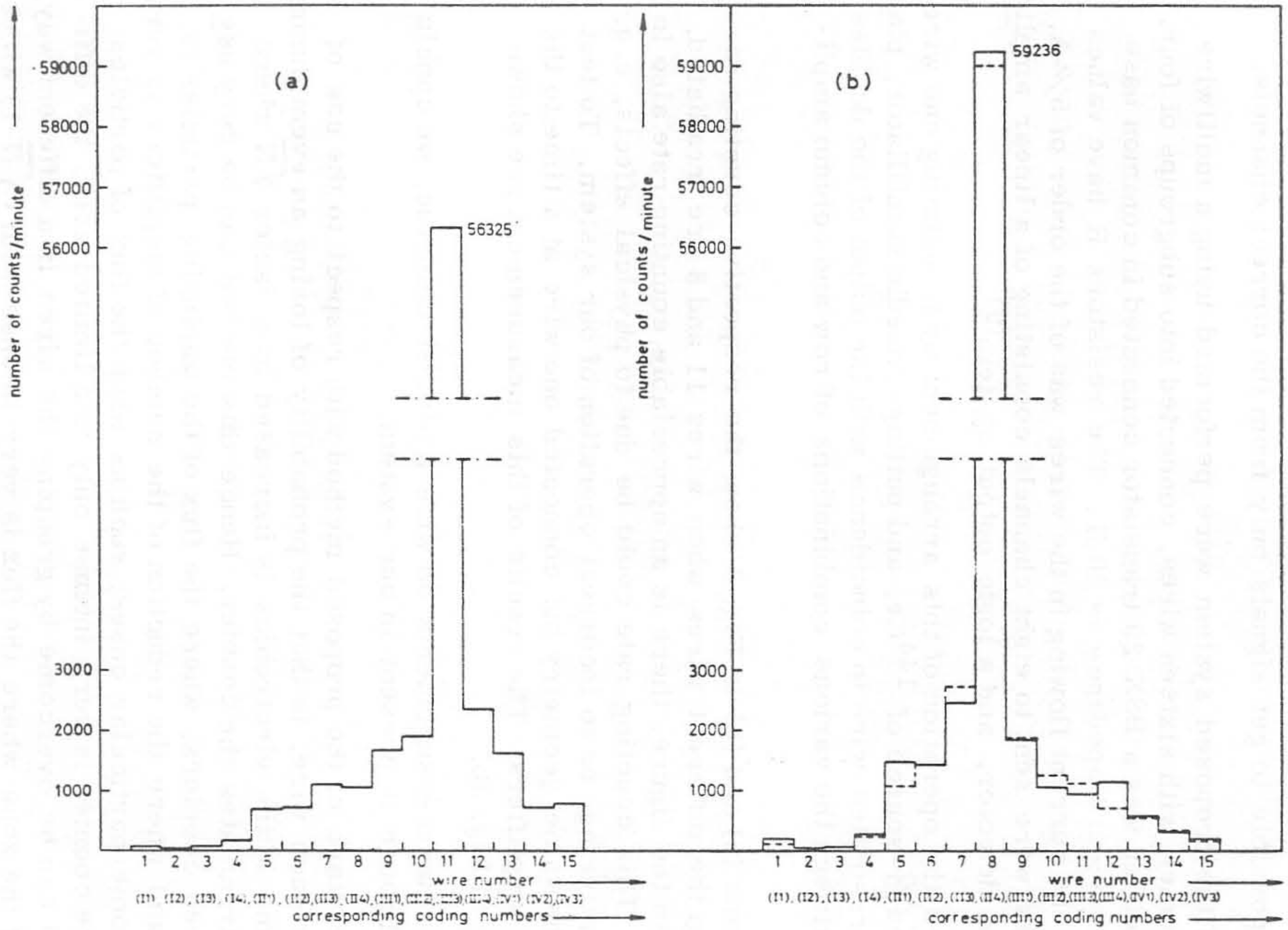

FIG. 3 - Counting rates measured on the different wires when: a) the wire 11 was irradiated; b) the wire 8 was irradiated (continuous line). Wire 8 was irradiated (dotted line) but only one wire at a time was connected to the row and column amplifiers. In all the measurements, wire 16 was not activated. The wire spacing was 3 mm, the diameter 20 μm; the filling gas (argon) was bubbled through ethyl alcohol.

2.4. - Instrumental energy resolution.-

With the described magnetic spectrometer, we expect a momentum resolution $\Delta p/p$ less than 3×10^{-3}. Thus for a K^- of 400 MeV/c we obtain an energy resolution of less than 0.75 MeV, and for a π^- of 430 MeV/c an energy resolution of less than 1.3 MeV.

2.5. - Beam contamination.-

As mentioned before, the slow K^- beam is heavily contaminated by π^- (50 π^- for one K^-), and one of the major difficulties is the elimination of the π^- in the trigger. In order to achieve this, we propose to use two lucite Čerenkov counters of the Fitch type, $\check{C}_1$ and $\check{C}_2$, placed in front of the first beam scintillator C_1 and behind the first MPWC of the magnetic spectrometer. The refractive index for lucite is 1.5, and K^- of 400 MeV/c do not give Čerenkov light; on the other hand, π^- (and also μ^- and e^-) of 400 MeV/c produce Čerenkov light. Thus a coincidence $C_1 \overline{\check{C}_1 \check{C}_2}$ will characterize a K^-. With this arrangement and using a radiator thickness of $\sim$5 cm, we expect a π^- rejection power from 10^{-3} to 10^{-4}. We need a further recognition of the K^- before the first magnetic analysis and behind the target in order to reduce the number of π^- in the beam that are not recognized by the first arrangement, and to eliminate the π^- arising from K^- decays in flight in the magnet. It seems dangerous to set up a third Čerenkov counter, because it introduces a considerable amount of matter (we need ~ 1 g/cm^2 of lucite to have an efficiency of 98-99%). It seems better to use three scintillator counters C_2, C_3, C_4, each 2 mm thick (see Fig. 4) and to distinguish K^- from π^- by pulse-height analysis.

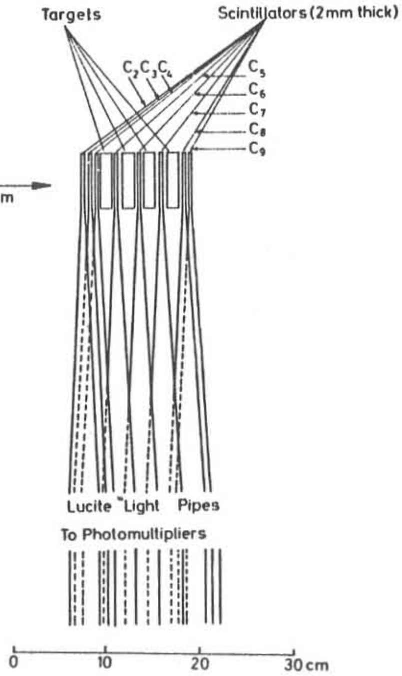

FIG. 4 - View of the sandwiched target.

Figure 5a gives the energy loss distributions for π^- and K^- of 400 MeV/c in a 2 mm thick scintillator. Figure 5b gives the probability of obtaining from a π^- traversing the scintillator, an energy loss greater than a certain value which corresponds to an electronic bias, as a function of this bias. We see that by fixing the threshold at a value which is half-way between the more probable values of the energy losses of π^- and K^-, the probability that a π^- gives an energy loss greater than bias is $\sim 7\%$. Thus the probability that a π^- gives an energy loss greater than the threshold in all the three scintillators is $(7\text{x}10^{-2})^3$, i.e. $\sim 5\text{x}10^{-4}$.

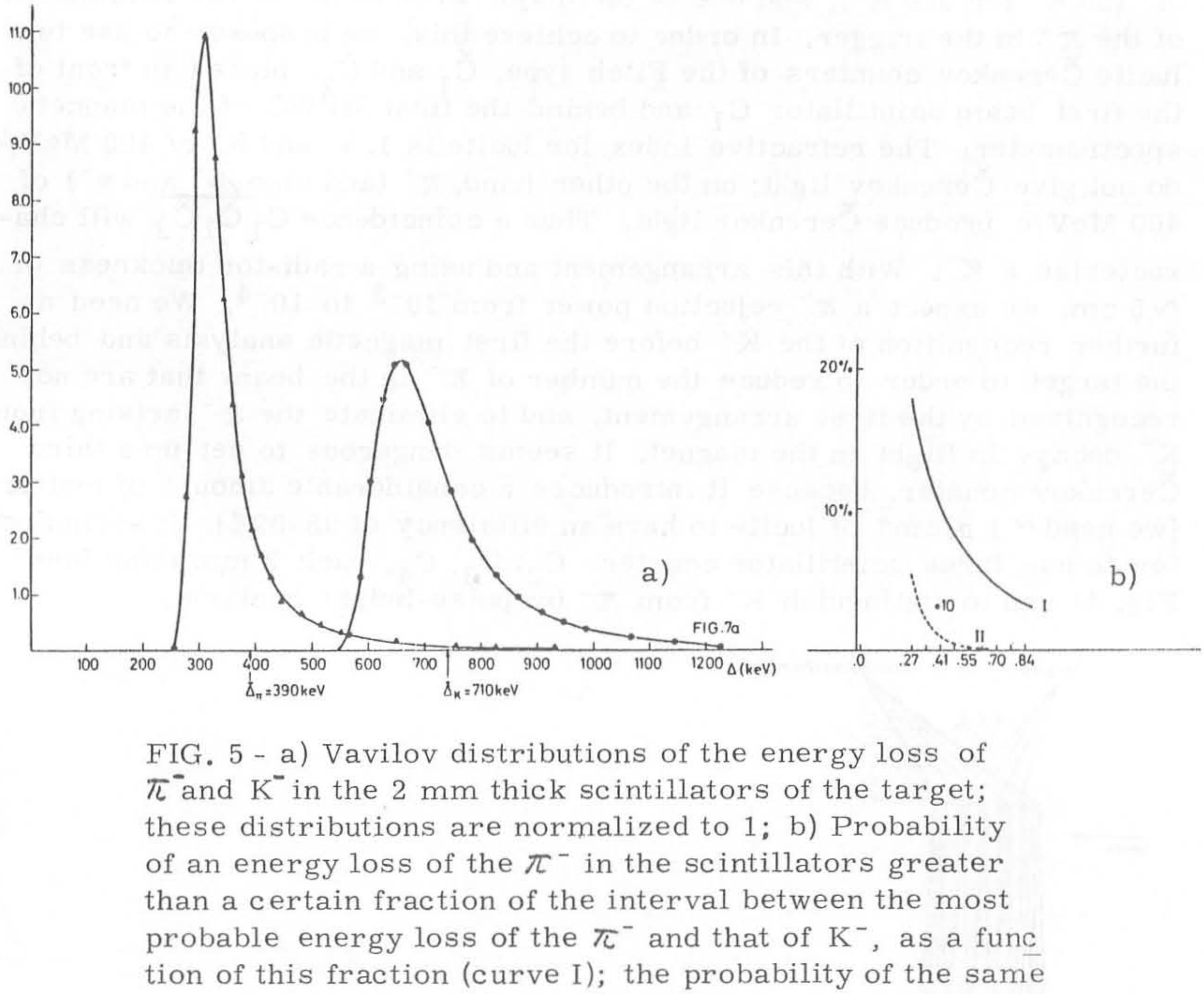

FIG. 5 - a) Vavilov distributions of the energy loss of π^- and K^- in the 2 mm thick scintillators of the target; these distributions are normalized to 1; b) Probability of an energy loss of the π^- in the scintillators greater than a certain fraction of the interval between the most probable energy loss of the π^- and that of K^-, as a function of this fraction (curve I); the probability of the same event for three scintillators (curve II).

In the same way, we use two scintillators before the target in order to select the emerging π^-. An event in which a K^- has struck the target and a π^- has emerged in the forward direction, will be signalled by a $C_1 \overline{\check{C}}_1 \overline{\check{C}}_2 \overline{C}_2 \overline{C}_3 \overline{C}_4 C_8 C_9 C_{10}$ coincidence, which is the trigger for the MPWC. Figure 6 gives a schematic block diagram of the electronics.

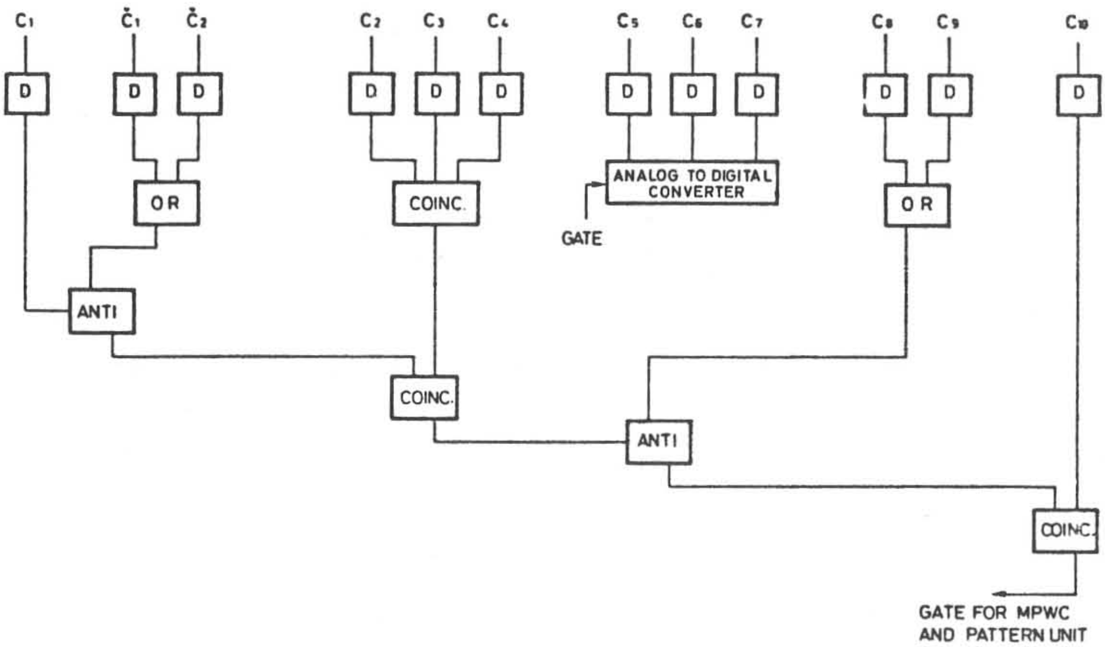

FIG. 6 - Schematic block diagram of the electronics.

2.6.- Spurious events.-

The trigger signal may be given by other events. Assuming that we will have 10^4 K^-/burst, 50 π^- for one K^-, and a π^- rejection power of 10^6, we expect to have 0.5 events/burst owing to this lack of efficiency grouped in a narrow peak. This peak will be displaced by $\sim$20-30 MeV/c from the π^- coming from the true reaction (1).

A trigger signal will be also given by the 3.6% of K^- which decay in flight along the distance between C_2, C_3, C_4 and C_8, C_9 ($\sim$10 cm). The following remarks are pertinent to this problem:

i) The two-body decays of the K^- ($K^- \to \mu^- + \bar{\nu}$ and $K^- \to \pi^- + \pi^0$), which total a relative abundance of 84.4%, are not dangerous, because only the momenta of particles lower than $\sim$430 MeV/c can be analysed in our apparatus, in a cone centered at 0^o and with an aperture of 6^o. Figure 7 shows the momenta of the μ^- and the π^- from the two-body decays as a function of the emission angle, for $p_k = 400$ MeV/c. We can see that the μ^- momenta are considerably greater than the momenta of the π^- from the reaction (1), and also the momenta of π^- arising from K^- decays are, within the angular range of 6^o, greater by almost 20 MeV/c than those of the π^- from the reaction (1).

The r.m.s. projected angle due to multiple Coulomb scattering in the target is of the order of 30', so this effect changes the above values only negligibly.

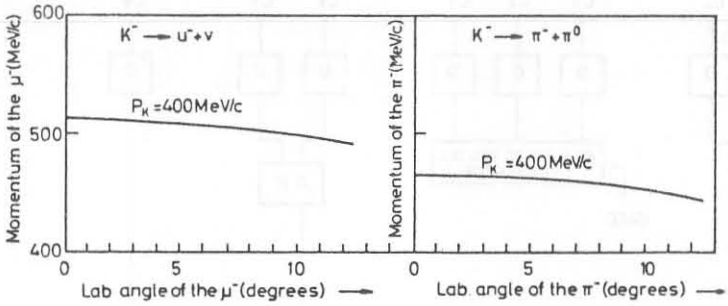

FIG. 7 - Momenta of the μ^- from the decay $K^- \to \mu^- + \overline{\nu}$ and of the π^- from the decay $K^- \to \pi^- + \pi^0$ as a function of their emission angle for $p_k =$ $= 400$ MeV/c.

ii) The three π decay ($K^- \to \pi^- + \pi^- + \pi^+$, $K^- \to \pi^- + \pi^0 + \pi^0$) cannot feed the region of interest, because the maximum momentum is 335 MeV/c.

iii) The decays $K^- \to \mu^- + \pi^0 + \overline{\nu}$ and $K^- \to e^- + \pi^0 + \overline{\nu}$ can introduce in the interesting region a continuous spectrum.

Using a Monte Carlo calculation, we have evaluated the number of events with momentum greater than 410 MeV/c arising from these decays, and found 330 events/day for the e^- decay and 466 events/day for the μ^- decay. We think that these events, broadened in a flat spectrum, do not seriously affect the energy spectrum of the true events. If necessary, they would be diminished by surrounding the target with lead-glass Čerenkov counters in anticoincidence, for detecting the γ-rays from the decay of the associated π^0.

The background not eliminated by the counter system will be measured by running the experiment with an empty target.

2.7. - Targets. -

The target thickness must be chosen taking into account the two conflicting features, i.e. that an increase of the thickness enhances the number of events but worsens the resolution. The degradation of the energy resolution by the target thickness is due to the following effects:

i) Differences of energy losses of the K^- and π^- in the target. -

The difference between the mean specific ionization dE/dx of K^- and π^- of 400 MeV/c is about 90% of the dE/dx of the π^-, as can be seen from Fig. 5. So the uncertainty with respect to the energy loss, without detection of the interacting point along the beam axis, is too much for a target of 5 g/cm^2. Therefore we must use a 5 g/cm^2 thick target which is sandwiched between 2 mm thick scintillators in order to measure the dE/dx of the particles at different thickness of the target. Figure 4 gives a sketch of this arrangement. With the three scintillators C_5, C_6, and C_7 we can divide the target into four sheets, and can recognize the sheet in which the reaction occurred by digitalizing and analysing the pulse height in the scin tillators. We will obtain an uncertainty $\Delta E_1 \simeq 1.8$ MeV (FWHM) on the energy loss in the target.

ii) Fluctuation of the energy losses of the K^- and π^- in the target and in the scintillators. -

We can calculate that the straggling of K^- and π^- in the sandwiched target introduces an uncertainty $\Delta E_2 \simeq 2.0$ MeV (FWHM) on the peak of the energy loss around its most probable value. One can think that if a reduction of the true counting rates is acceptable, a non-sandwiched target of 1 g/cm^2 would diminish the straggling considerably. On the other hand, the amount of matter of the five scintillators C_2, C_3, C_4, C_8 and C_9 is also 1 g/cm^2, so the number of events produced in the scintillators would be of the same order as the number of events in the targets.

2.8.- Total energy resolution.-

Taking into account the instrumental energy loss and the uncertainties introduced by the target thickness, one expects a total energy resolution of ~ 3.0 MeV for the detection of hypernuclear levels. This resolution is sufficient to give a first insight into the hypernuclear levels which are excited. For more detailed studies, a set of solid-state counters will be placed around the target to detect the low-energy γ-rays arising from the decay of the hypernuclear levels. Fig. 8 gives a pictorial view of the experimental set-up.

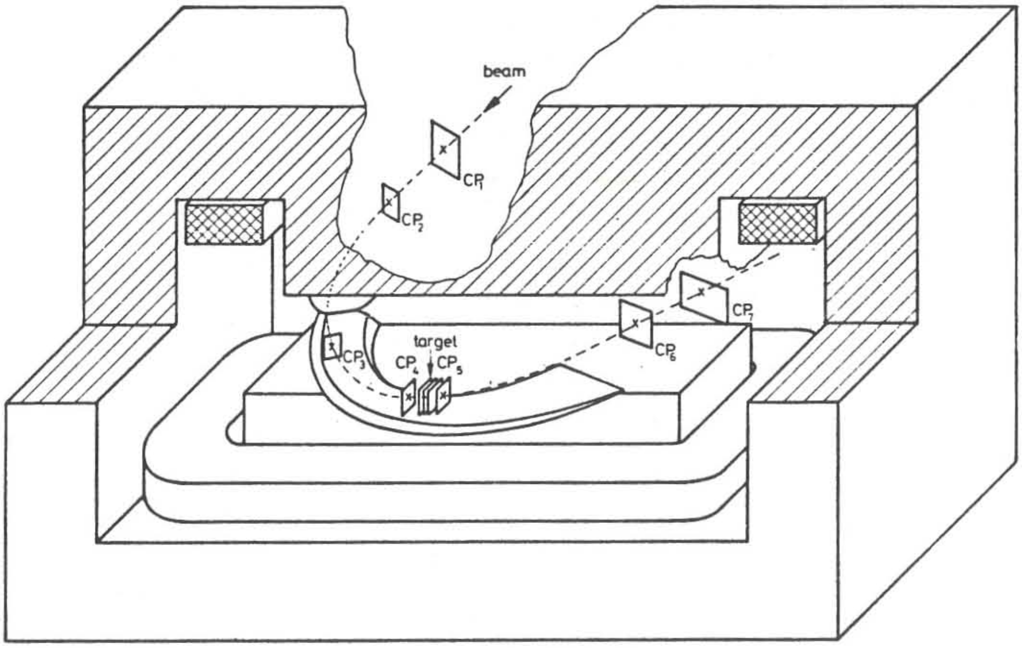

FIG. 8 - Pictorial view of the experimental set-up.

2.9. - Computer. -

It will be necessary to use an on-line computer to read the MPWC; we plan to use a PDP 11 computer, which will be suitable for our purposes. The events will be stored on a magnetic tape for the subsequent off-line analysis, and for this we will use a Kennedy incremental tape unit.

REFERENCES. -

(1) - G.C. Bonazzola, T. Bressani, E. Chiavassa, S. Costa, L. Ferrero, L. Pasqualini, G. Rovero, G. Venturello and C. Rubbia, Internal document CERN PH III-70/5 (1970).

(2) - T. Bressani, E. Chiavassa and C. Rubbia, Report INFN/BE-70/4 (1970).

(3) - H. Feshbach and A.K. Kerman, in Preludes in Theoretical Phys., editors A. De-Shalit, H. Feshbach and L. Van Hove (North-Holland Pub. Co., Amsterdam 1966), p. 260.

(4) - R.H. Dalitz, Proc. Intern. Conf. on Hypernuclear Phys., Argonne (1969), p. 708.

(5) - CERN-Heidelberg-Warsaw group, Internal document CERN PH III-70/8 (1970).

(6) - G.C. Bonazzola, T. Bressani, E. Chiavassa, V.I. Tricomi and C. Rubbia, paper presented at the Intern. Conf. on Instrumentation for High-Energy Phys., Dubna (1970).

(7) - I. Pizer, in Proc. Informal Meeting on Filmless Spark Chamber Techniques and Associated Computer Uses, CERN 64-30 (1964), p. 111.

(8) - G. Charpak, R. Bouclier, T. Bressani, J. Favier and Č. Zupančič, Nuclear Instr. and Meth. 65, 217 (1968).

(9) - C. Tarlè and H. Verweij, Nuclear Instr. and Meth. 78, 93 (1970).